Motion Control of Passive Intelligent Walker Using Servo Brakes

doi: 10.1109/TRO.2007.906252

Motion Control of Passive Intelligent Walker Using Servo Brakes

Yasuhisa Hirata, *Member, IEEE*, Asami Hara, and Kazuhiro Kosuge, *Fellow, IEEE*

***Abstract*—We propose a new intelligent walker based on passive robotics that assists the elderly, handicapped people, and the blind who have difficulty in walking. We developed a prototype of the Robot Technology Walker (RT Walker), a passive intelligent walker that uses servo brakes. The RT Walker consists of a support frame, two casters, two wheels equipped with servo brakes, and it has passive dynamics that change with respect to applied force/moment. This system is intrinsically safe for humans, as it cannot move unintentionally, i.e., it has no driving actuators. In addition, the RT Walker provides a number of navigational features, including good maneuverability, by appropriately controlling the torque of servo brakes based on RT. We propose a human adaptive motion control algorithm that changes the apparent dynamics to adapt to user difficulties, and an environmentally adaptive motion control algorithm, which incorporates environmental information to provide obstacle/step avoidance and gravity compensation functions. The proposed control algorithms are experimentally applied to the RT Walker to test their validity.**

***Index Terms*—Brake control, intelligent walker, passive robotics, physical interaction, robot technologies (RTs).**

I. Introduction

AS SOCIETIES age and experience a shortage of people for nursing care, handicapped people, including the elderly and blind, find it increasingly necessary to be self-supporting. However, many such people suffer from injuries, poor eyesight, or a general lack of muscular strength, and need the support of other people in daily activities. In the living environment, the ability to walk is one of the most important and fundamental functions for humans, and enables them to realize high-quality lives.

This paper focuses on a walker-type support system, which works on the basis of the physical interaction between the system and the user. Walkers are widely used by the handicapped because they are simple and easy to use. Many robotics researchers have considered improving their functionality by adding wheels with actuators and controlling them based on robot technology (RT), such as motion control technology, sensing technology, vision technology, and computational intelligence.

Fujie *et al*. developed a power-assisted walker for physical support during walking [1]. We developed a motion control algorithm for an intelligent walker with an omnidirectional mobile base, in which the system is moved based on the user's intentional force/moments [2]. Manuel *et al*. proposed a nonholonomic navigation system for a walking-aid robot named Care-O-bot II [3]. Sabatini *et al*. developed a motorized rollator [4]. Yu *et al*. proposed the Personal Aid for Mobility and Monitoring (PAMM) system to provide mobility assistance and user health status monitoring [5]. Kotani *et al*. proposed the HITOMI system, which helps the blind navigate outdoors [6]. In [7], various assisting technologies are surveyed, and some electric intelligent walkers are introduced.

Many intelligent walkers based on RT consist of servo motors mounted on a mobile base and sensors such as force/torque and ultrasonic sensors. Information from many types of sensors controls the servo motors. By appropriately controlling the servo motors, these intelligent walkers provide many functions, such as variable motion, obstacle avoidance, and navigation; thus, they provide a maneuverable system that supports walking.

On the other hand, simple walkers without servo motors consisting of a frame, wheels or casters, and hand brakes, are well known and commercially available. People can use these walkers intuitively, because they move these systems passively using intentional force/moment. However, unlike active intelligent walkers that employ servo motors, it is impossible to change the apparent dynamics of these systems; they are completely passive and cannot adapt to differing user difficulties. In addition, these systems cannot move properly in an environment with obstacles or slopes, because they offer no environment-based control over their motion.

In this paper, we consider a passive intelligent walker, which is not only simple and safe but also offers many functions similar to those found in active walkers. We develop a passive intelligent walker called the RT Walker that uses servo brakes and incorporates passive robotics. First, we explain the concept of passive robotics, and introduce the passive intelligent walker. Then, we propose motion control algorithms that allow the walker to adapt to user characteristics and move based on information about its environment, and evaluate the validity of these motion control algorithms through several experiments.

II. Passive Robotics

For practical use of intelligent systems in the real world, we need to consider two main points: achieving high performance and user safety. Most conventional intelligent systems have servo motors that are controlled based on sensory information from sensors such as force/torque and ultrasonic sensors. The high performance of intelligent systems is realized in the

Manuscript received October 9, 2006; revised May 21, 2007. This paper was recommended for publication by Associate Editor C. Laschi and Editor H. Arai upon evaluation of the reviewers' comments.

Y. Hirata and K. Kosuge are with the Department of Bioengineering and Robotics, Tohoku University, Sendai 980-8579, Japan (e-mail: hirata@irs.mech.tohoku.ac.jp, kosuge@irs.mech.tohoku.ac.jp).

A. Hara was with the Department of Bioengineering and Robotics, Tohoku University, Sendai 980-8579, Japan. She is now with JTEKT Corporation, Kariya 448-8652, Japan.

Color versions of one or more of the figures in this paper are available online at http://ieeexplore.ieee.org.

Digital Object Identifier 10.1109/TRO.2007.906252

form of functions such as power assistance, collision avoidance, navigation, and variable motion.

However, if we cannot appropriately control the servo motors, they can move unintentionally, and might be dangerous for a human being. In particular, in Japan, legislation must be formulated for using them in a living environment. In addition, active intelligent systems tend to be heavy and complex because they require servo motors, reduction gears, sensors, a controller, and rechargeable batteries. Batteries present a significant problem for long-term use because servo motors require a lot of electricity.

Goswami *et al*. proposed the concept of passive robotics [8], in which a system moves passively based on external force/moment without the use of actuators, and used a passive wrist comprising springs, hydraulic cylinders, and dampers. The passive wrist responds to an applied force by computing a particular motion and changing the physical parameters of the components to realize the desired motion. Peshkin *et al*. also developed an object handling system referred to as Cobot [9] consisting of a caster and a servo motor for steering the caster based on passive robotics.

Wasson *et al*. [10], Alwan *et al*. [11], and Rentschler *et al*. [12] proposed passive intelligent walkers. In most of these walkers, a servo motor is attached to the steering wheel, similar to the Cobot system, and the steering angle is controlled depending on environmental information. The RT Walker proposed in this paper also has passive dynamics with respect to the force/moment applied. It differs from other passive walkers in that it controls servo brakes appropriately without using any servo motors. These passive systems are intrinsically safe because they cannot move unintentionally. Thus, passive robotics will prove useful in many types of intelligent systems through physical interaction between the systems and humans.

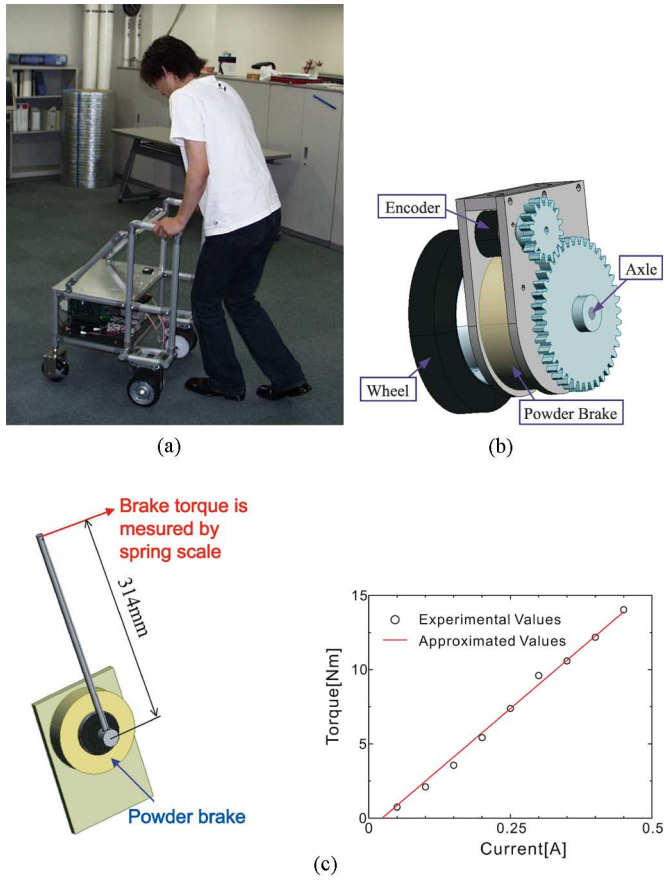

Fig. 1. Passive intelligent walker, referred to as the RT Walker, which provides control functions based on servo brake control. The servo brake generates brake torque depending on the input current. (a) Prototype of RT Walker. (b) Wheel with servo brake. (c) Characteristic of servo brake investigated by spring scale.

III. RT Walker

Conventional passive intelligent walkers consist of a frame for supporting the user's weight, a steering wheel, manual or automatic brakes, and sensors for detecting environmental information. A steering-wheel actuator is used for navigation in the environment. Brake systems such as hand brakes or automatic brakes limit the speed of the walker and prevent the user from falling. These functions, in particular, are important and essential for the safety of users.

In this research, we pay special attention to the braking system, and propose a new passive intelligent walker (RT Walker), which uses servo brake control. It differs from conventional passive intelligent walkers in that it does not have servo motors for steering. However, the servo brakes can navigate the RT Walker, and its maneuverability can change based on environmental information or the difficulties and conditions faced by the user.

The developed RT Walker is shown in Fig. 1(a). This prototype consists of a support frame, two passive casters, two wheels with servo brakes (referred to as powder brakes), a laser range finder, tilt angle sensors, and a controller. The part of the rear wheel with the powder brake is shown in Fig. 1(b); the brake torque is transferred directly to the axle. For controlling the brake torque, we investigate the actual torque of the powder brake by removing the brake from the wheel and measuring its actual torque with a spring scale, as shown in Fig. 1(c). As shown in Fig. 1(c), the brakes change the torque almost in proportion to the input current. We use values derived from the experimental results by least squares estimation.

RT Walker is lightweight because its structure is relatively simple compared to active intelligent walkers, and it needs little electricity to operate the servo brakes. The driving force of the RT Walker is the actual force/moment applied by the user, and therefore, he/she can move it passively without using the force/torque sensor. By changing the torque of the two rear wheels appropriately and independently, we can control the motion of the RT Walker, which receives environmental information from its laser range finder and tilt angle sensors. Based on this information, the RT Walker can realize the collision avoidance, gravity compensation, and other functions.

The servo brake and laser range finder are relatively expensive; however, they are high-performance components intended for industrial fields. In the welfare fields, human-assistance devices do not require high precision motions, and the part costs could be reduced if they are designed for the human support systems. Therefore, from the viewpoint of safety and cost effectiveness, the RT Walker will be used in the near future.

IV. Motion Control Algorithm

Realizing the many functions of the RT Walker is challenging, because we control only the servo brakes and use no servo motors. In this section, we explain servo brake control and propose a fundamental motion control algorithm of the RT Walker. We propose two motion control algorithms based on the fundamental algorithm: human adaptive and environmentally adaptive motion control.

A. Motion Control of the RT Walker Based on Servo Brakes

First, we explain the relationships among brake torque, angular velocity, and applied torque of the wheels with servo brakes. The RT Walker moves based on only the external force/moment applied to it, because it does not have any actuators such as servo motors. To control the motion of the RT Walker based on the external force f_{ew} applied to the wheel with a servo brake, we can derive the following relationships with respect to the angular velocity of the wheel with servo brakes ω_w:

$$\text{for} \quad \omega_w \neq 0, \qquad t_{bw} = -k_b I_b \,\mathrm{sgn}(\omega_w) \tag{1}$$

$$\text{for} \quad \omega_w = 0, \qquad t_{bw} = \begin{cases} -f_{ew} R_w, & |f_{ew}| R_w \leq k_b I_b \\ -k_b I_b \,\mathrm{sgn}(f_{ew}), & |f_{ew}| R_w > k_b I_b \end{cases} \tag{2}$$

where t_{bw} is the brake torque generated by the servo brake, R_w is the radius of the wheel, I_b is the input current for the servo brakes, and k_b is the positive coefficient expressing the relationship between the brake torque and the input current. Unlike servo motor control, we can control the motion of the RT Walker by considering only these relationships.

Next, we describe the RT Walker's fundamental motion control algorithm. Under the assumption that the center of mass m of the RT Walker is in the middle of the wheels with powder brakes, as shown in Fig. 2, the damping coefficient is defined as D, the inertial moment and the damping coefficient around the center of mass are defined as J and D_θ, respectively, and the velocity and the acceleration are defined as $\dot{\mathbf{q}}$ and $\ddot{\mathbf{q}}$, respectively. The RT Walker's dynamics, based on the force/moment $\tau_{\mathbf{h}} = [f_h, n_h]^T$ applied by a human and the brake force/moment $\tau_{\mathbf{b}} = [f_b, n_b]^T$ generated by the powder brakes, is expressed as follows:

$$\mathbf{M}\ddot{\mathbf{q}} + \mathbf{D}\dot{\mathbf{q}} = \mathbf{E_h}\tau_{\mathbf{h}} - \mathbf{E_b}\tau_{\mathbf{b}}$$

$$\mathbf{M} = \begin{bmatrix} m & 0 & 0 \\ 0 & J & 0 \\ 0 & 0 & m \end{bmatrix}, \quad \mathbf{D} = \begin{bmatrix} D & 0 & 0 \\ 0 & D_\theta & 0 \\ 0 & 0 & D \end{bmatrix}, \quad \mathbf{q} = \begin{bmatrix} {}^o x \\ \theta \\ {}^o y \end{bmatrix}$$

$$\tau_{\mathbf{h}} = \begin{bmatrix} f_h \\ n_h \end{bmatrix}, \qquad \tau_{\mathbf{b}} = \begin{bmatrix} f_b \\ n_b \end{bmatrix}, \qquad \mathbf{E_h}, \mathbf{E_b} = \begin{bmatrix} \cos\theta & 0 \\ 0 & 1 \\ \sin\theta & 0 \end{bmatrix} \tag{3}$$

where $\mathbf{M} \in R^{3\times3}$ is the inertia matrix and $\mathbf{D} \in R^{3\times3}$ is the damping matrix. In this research, the brake force/moment $\tau_{\mathbf{b}} = [f_b, n_b]^T$ generated by the brakes is controlled for realizing an arbitrary motion of the RT Walker, and we derive the brake torque $\mathbf{t_b} = [t_{br}, t_{bl}]^T$ for each wheel as

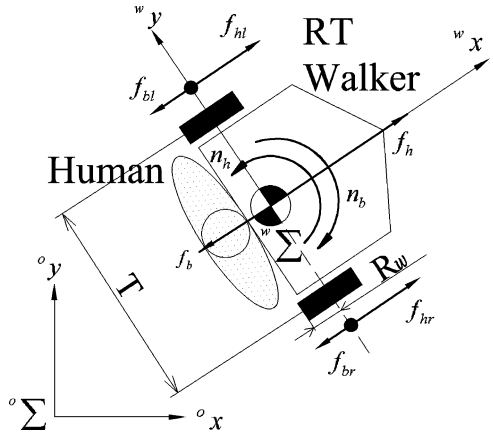

Fig. 2. Model of the RT Walker used to design the motion control algorithm, in which the center of mass is in the middle of the wheels with powder brakes.

$$\mathbf{t_b} = \begin{bmatrix} t_{br} \\ t_{bl} \end{bmatrix} = \begin{bmatrix} R_w/2 & R_w/T \\ R_w/2 & -R_w/T \end{bmatrix} \begin{bmatrix} f_b \\ n_b \end{bmatrix} \tag{4}$$

where T is the distance between the wheels with powder brakes.

B. Human Adaptive Motion Control Algorithm

If we can change the apparent dynamics of the RT Walker based on the many kinds of difficulties the users face, we can improve its maneuverability and make it suitable as a rehabilitation system by increasing the load using the brake control. A fall-prevention function could be realized by changing the apparent dynamics of the RT Walker in real time based on the user's situation. The fall-prevention function is very important for walker users.

In this section, we discuss a motion control algorithm for variable dynamics of the RT Walker. The dynamics of the RT Walker are expressed by (3), and we consider the apparent dynamics of an RT Walker expressed as follows:

$$\mathbf{M_d}\ddot{\mathbf{q}} + \mathbf{D_d}\dot{\mathbf{q}} = \mathbf{E_h}\tau_{\mathbf{h}}$$

$$\mathbf{M_d} = \begin{bmatrix} m_d & 0 & 0 \\ 0 & J_d & 0 \\ 0 & 0 & m_d \end{bmatrix}, \qquad \mathbf{D_d} = \begin{bmatrix} D_d & 0 & 0 \\ 0 & D_{\theta d} & 0 \\ 0 & 0 & D_d \end{bmatrix} \tag{5}$$

where $\mathbf{M_d} \in R^{3\times3}$ is the apparent inertia matrix of the RT Walker and $\mathbf{D_d} \in R^{3\times3}$ is the apparent damping matrix. If we can change these parameters, we can realize many motion characteristics with the RT Walker.

The RT Walker has a nonholonomic velocity constrain expressed as

$${}^o\dot{x} \sin\theta - {}^o\dot{y} \cos\theta = 0. \tag{6}$$

By adding this nonholonomic constraint to (3) and (5), and by reducing the order with respect to $\dot{\mathbf{q}}$, $\ddot{\mathbf{q}}$ [13], we derive the following equation with respect to the brake force/moment $\tau_{\mathbf{b}} =$

$[f_b, n_b]^T$:

$$\tau_{\mathbf{b}} = \begin{bmatrix} f_b \\ n_b \end{bmatrix} = \begin{bmatrix} \frac{m_d - m}{\cos\theta}{}^o\ddot{x} + \frac{1}{\cos\theta}[(m_d - m)\dot{\theta}\tan\theta + D_d - D]^o\dot{x} \\ -(J_d - J)\ddot{\theta} - (D_{\theta d} - D_\theta)\dot{\theta} \end{bmatrix}. \tag{7}$$

When we derive the brake force/moment $\tau_{\mathbf{b}} = [f_b, n_b]^T$ from (7), and specify the brake torque of the powder brakes in (4), RT Walker can move as if it has the apparent dynamics expressed by $\mathbf{M_d}$ and $\mathbf{D_d}$ in (5). Therefore, we can vary the mobility characteristics of the RT Walker according to the difficulties faced by the users or their conditions. The methods for defining suitable apparent dynamics for the user are part of the research on human–robot cooperation. In the future, we will introduce this research to the control of the passive intelligent walker.

The prototype developed in this research could not provide accurate acceleration feedback because it has only a low-resolution encoder for each wheel to calculate its acceleration. Therefore, to use the RT Walker, we assume that $\mathbf{M_d}$ is equal to $\mathbf{M}$, and modify (7) as the following equation; however, the apparent inertia matrix could not be changed in this case:

$$\tau_{\mathbf{b}} = \begin{bmatrix} f_b \\ n_b \end{bmatrix} = \begin{bmatrix} \frac{D_d - D}{\cos\theta}{}^o\dot{x} \\ -(D_{\theta d} - D_\theta)\dot{\theta} \end{bmatrix}. \tag{8}$$

Note that, if we use high-resolution encoders or acceleration sensors to detect the correct acceleration of the RT Walker, we can change both the apparent inertia matrix and the apparent damping matrix of the RT Walker expressed in (5) under the relationship expressed in (1) and (2).

C. Environmentally Adaptive Motion Control Algorithm

When we use intelligent walkers in living environments, we must consider motion control algorithms based on information about the environment. In particular, in environments with differences in the street level, stairs, or many obstacles or slopes, using walkers safely and smoothly requires environmentally adaptive motion control.

To realize an environmentally adaptive motion control algorithm, we modify (3) as follows:

$$\mathbf{M}\ddot{\mathbf{q}} + \mathbf{D}\dot{\mathbf{q}} + \mathbf{G} = \mathbf{E_h}\tau_{\mathbf{h}} - \mathbf{E_b}\tau_{\mathbf{b}} \tag{9}$$

where $\mathbf{G}$ is the gravity applied to the RT Walker. By controlling the brake torque of each wheel for avoiding the collision with obstacles or missing steps, we realize the following apparent dynamics of the RT Walker:

$$\mathbf{M_d}\ddot{\mathbf{q}} + \mathbf{D_d}\dot{\mathbf{q}} = \mathbf{E_h}\tau_{\mathbf{h}} + \mathbf{E_r}\tau_r \tag{10}$$

where τ_r is the virtual force/moment generated based on environmental information. If the system derives the virtual force/moment based on the distance between obstacles/steps, and appropriately generates braking torque, a user could avoid collisions with obstacles or prevent missing his/her steps due to a difference in the level. By compensating for the force of gravity, the user could use it safely on any road, even with a steep slope, because it would not move based on the gravity on the slope. In the following section, we discuss how the virtual force/moment τ_r or the gravity effect $\mathbf{G}$ are generated and applied to the RT Walker as braking torque.

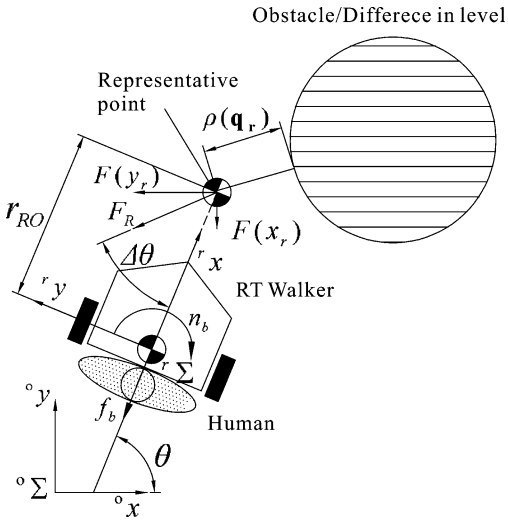

Fig. 3. Virtual force/moment is applied to the RT Walker based on the distance between the walker and the obstacle/step to avoid collision with obstacles or prevent tripping on stairs, steps, or differences in the street level.

1) Motion Control Based on Virtual Force/Moment: In this section, we derive the virtual force/moment generated based on environmental information to avoid collision with obstacles or falling down due to stairs, steps, and differences in street level. We use a method called artificial potential field, proposed by Khatib [14], which is generally used in research on robot collision avoidance.

We designed the artificial potential field $\mathbf{U}(\mathbf{q_r})$ based on the positions of obstacles or steps as follows:

$$\mathbf{U}(\mathbf{q_r}) = \begin{cases} k\left(1 + \cos\frac{\pi}{\rho_0}\rho(\mathbf{q_r})\right), & \rho(\mathbf{q_r}) \le \rho_0 \\ 0, & \rho(\mathbf{q_r}) > \rho_0 \end{cases} \tag{11}$$

where $\mathbf{q_r} = [x_r, \theta, y_r]^T$ is the position/orientation of the representative point on the front of the RT Walker, as shown in Fig. 3, k is the positive constant gain, $\rho(\mathbf{q_r})$ is the shortest distance from $\mathbf{q_r}$ to an obstacle/step, and ρ_0 is the limit distance of the potential field influence. From (11), $\mathbf{U}(\mathbf{q_r})$ is larger than zero and increases when RT Walker is close to obstacles or level differences. On the other hand, when $\rho(\mathbf{q_r})$ is larger than ρ_0, $\mathbf{U}(\mathbf{q_r})$ is equal to zero.

For controlling mobile robots, manipulators, etc., some researchers design an artificial potential field function with a value that reaches infinity when the robot is close to obstacles. However, in the case of walkers, the user may be closing on a place such as a door, a shelf, or an elevator. Therefore, in this research, we designed the artificial potential field with an upper limit of a potential value, such as (11). Using this type of an artificial potential field, the user can move the RT Walker close to these places by applying a large force/moment.

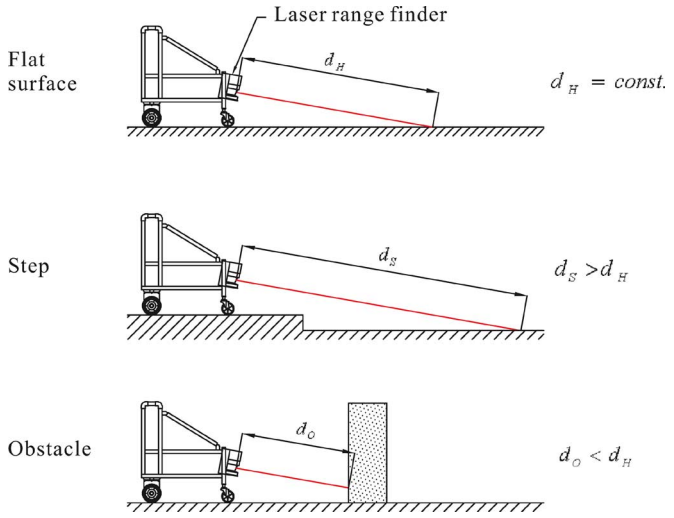

Fig. 4. Obstacle/step detection using the laser range finder. The RT Walker obtains the ground information based on the measured distances.

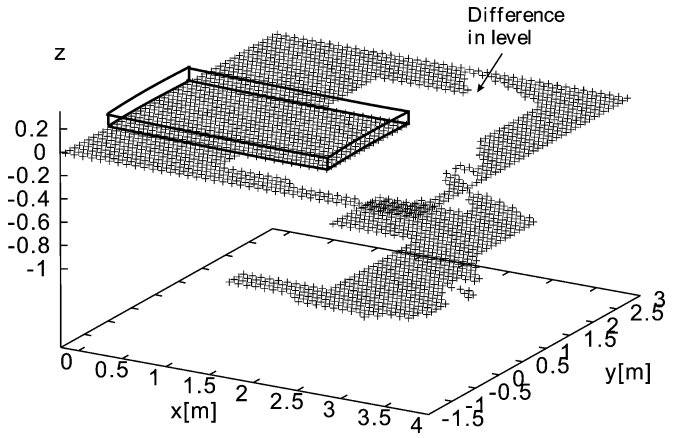

Fig. 5. Map information showing differences in ground level around the RT Walker, which are detected by the laser range finder.

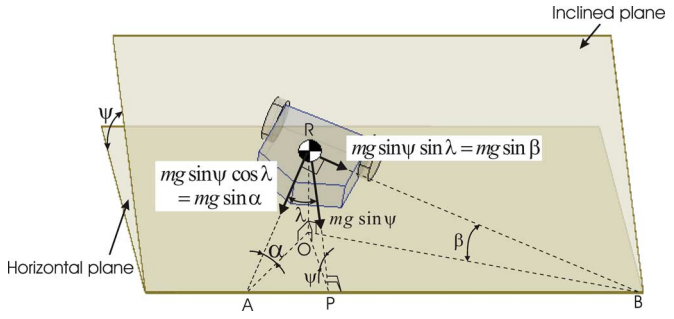

Fig. 6. Pitch and roll angles of the RT Walker with respect to the horizontal plane detected by two tilt angle sensors.

From (11), we generate the virtual force/moment applied to the walker's representative point as follows:

$$\mathbf{F}(\mathbf{q_r}) = -\nabla \mathbf{U} \tag{12}$$

where $\nabla \mathbf{U}$ is the gradient vector of $\mathbf{U}$ with respect to $\mathbf{q_r}$. From this equation, we can derive the virtual force $\mathbf{F}(\mathbf{q_r})$ applied to

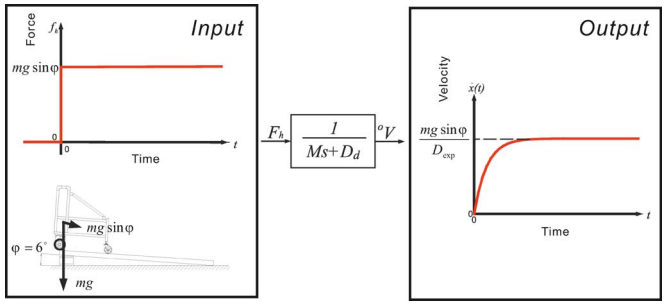

Fig. 7. Experiments using a slope for investigating variable motion characteristics. This experiment derived the velocity responses of the RT Walker along the heading direction.

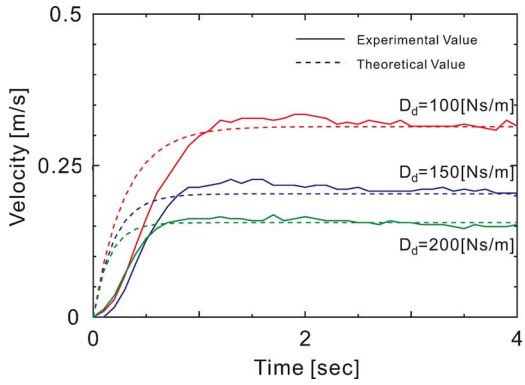

Fig. 8. Experimental results illustrating the velocity response of the RT Walker along its heading direction. Changing the damping coefficients of the RT Walker based on the brake control changed the velocity responses, and they converged to the desired damping coefficients.

TABLE I
DAMPING COEFFICIENT OF VELOCITY RESPONSE EXPERIMENTS

Desired Damping Coefficient $D_d[Ns/m]$	*Actual Damping Coefficient* $D_{exp}[Ns/m]$
100.00	94.89
150.00	146.29
200.00	203.95

the representative point of the RT Walker as follows:

$$\mathbf{F}(\mathbf{q_r}) = \begin{cases} \dfrac{k\pi}{\rho_0} \sin \dfrac{\pi}{\rho_0}\rho(\mathbf{q_r}) \cdot \rho(\mathbf{q_r}), & \rho(\mathbf{q_r}) \le \rho_\mathbf{0} \\ 0, & \rho(\mathbf{q_r}) > \rho_0. \end{cases} \tag{13}$$

From (13), we derive the virtual force/moment $\tau_\mathbf{r} = [f_r, n_r]^T$ applied to the center of mass of the RT Walker and the brake force/moment $\tau_\mathbf{b} = [f_b, n_b]^T$ as follows:

$$\tau_\mathbf{b} = \begin{bmatrix} f_b \\ n_b \end{bmatrix} = \begin{bmatrix} f_r \\ n_r \end{bmatrix} = \begin{bmatrix} -F_R \cos \Delta\theta \\ r_{RO} F_R \sin \Delta\theta \end{bmatrix} \tag{14}$$

where r_{RO} is the distance between the middle of axis of the real wheels and the representative point, and F_R and $\Delta\theta$ are expressed as

$$F_R = \sqrt{F^2(x_r) + F^2(y_r)}, \qquad \Delta\theta = \theta - \tan^{-1}\frac{F(y_r)}{F(x_r)}. \tag{15}$$

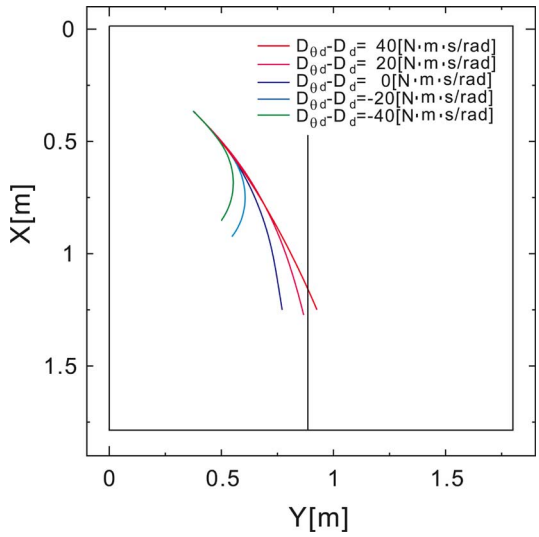

Fig. 9. Experimental results with respect to the rotational motion of the RT Walker on a slope. These results show the paths with different damping coefficients with respect to the rotational direction.

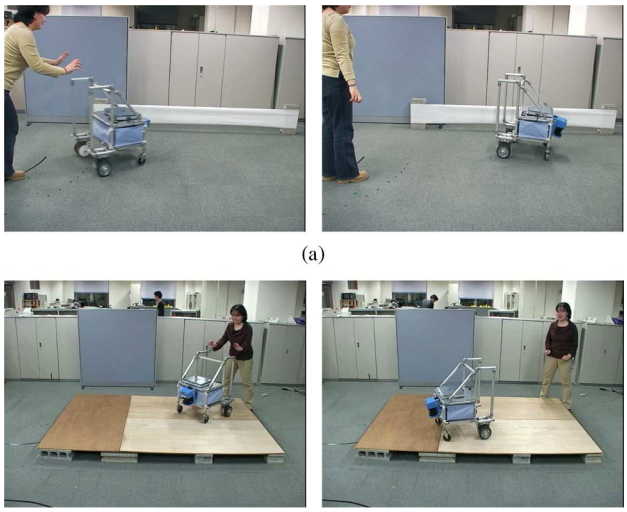

(a)

(b)

Fig. 10. Experimental results of avoiding obstacles or steps. In these experiments, the human pushes the walker just enough to move it, and it avoids the dangerous situations by controlling the servo brakes. (a) Avoidance motion for collision with obstacles. (b) Avoidance motion for steps.

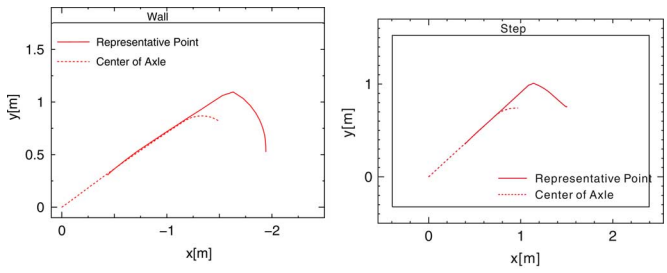

(a) (b)

Fig. 11. Experimental results showing the paths of the RT Walker in avoiding obstacles and steps. (a) Collision avoidance with obstacle. (b) Step avoidance motion.

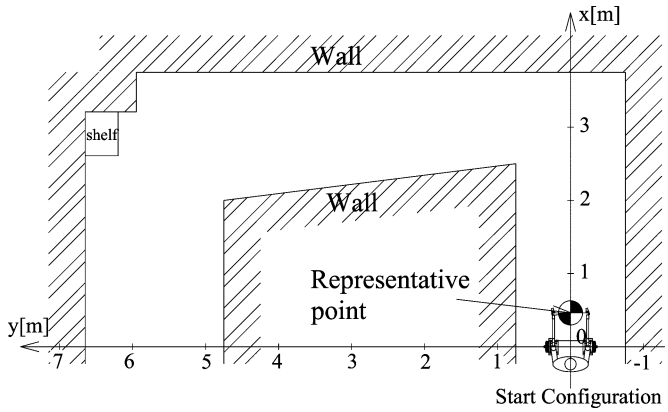

Fig. 12. Experimental setup in an environment with walls for investigating the validity of the environmentally adaptive motion control algorithm for collision avoidance.

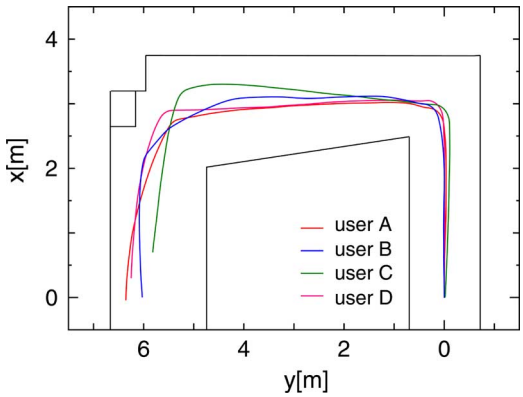

Fig. 13. Experimental results in an environment with walls. Four users, blindfolded to prevent visual feedback, walked using the RT Walker without colliding with the wall.

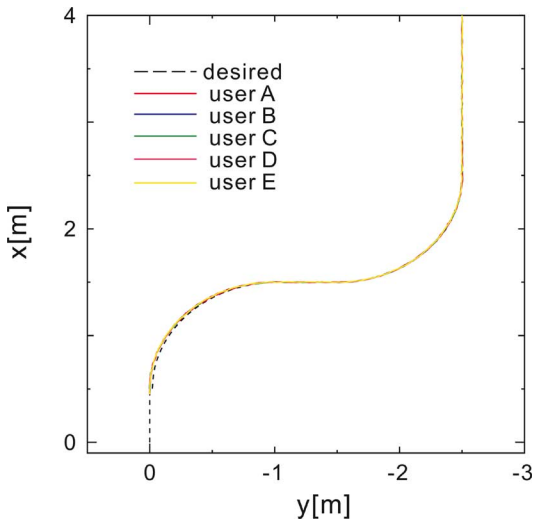

Fig. 14. Experimental results of path following. In this experiment, five blindfolded users operated the RT Walker and followed the path successfully.

Next, we measure the distance between the system and the obstacles or steps to derive the artificial potential field in the environment. In this research, we use the walker's laser range finder, which is attached at an angle to the horizontal plane, as

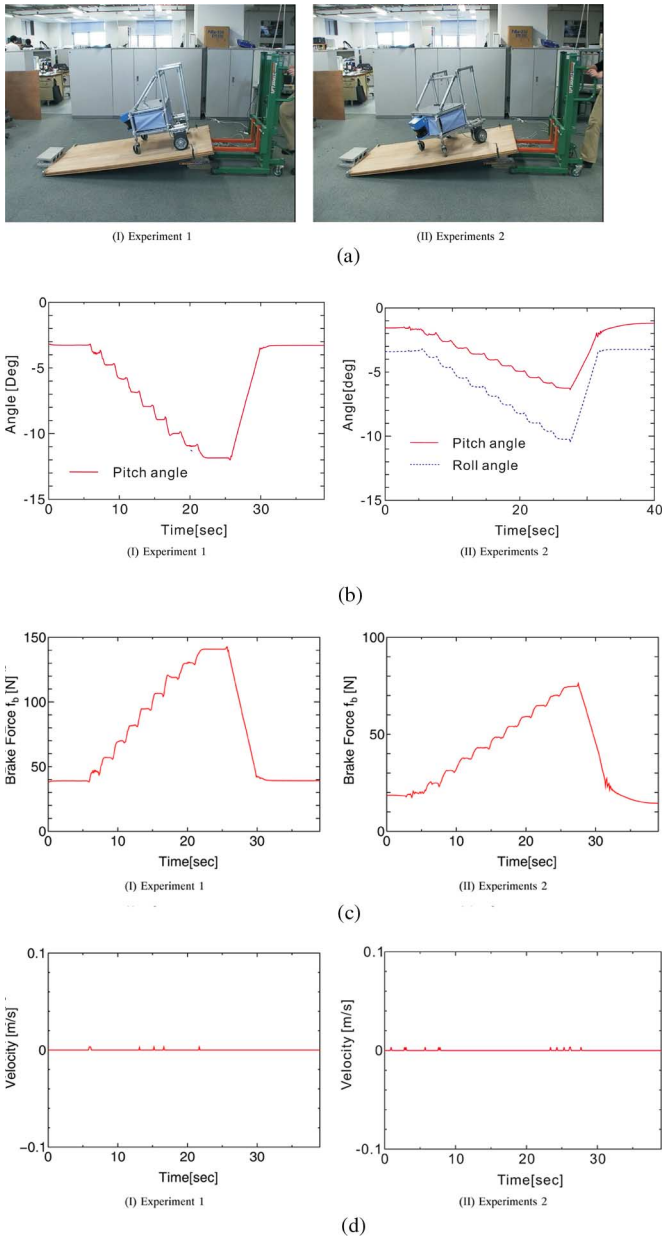

Fig. 15. Experimental results for gravity compensation. Two arrangements of the RT Walker with respect to the tilted plate are investigated, and both results showed that the RT Walker changed the brake force based on changes of its angle, compensating for the force of gravity. The RT Walker does not generate velocity even when its angle is changed. (a) RT Walker was tilted with a fork lift. (b) Angle of the RT Walker with respect to the horizontal plane. (c) Brake force generated by the servo brake, (d) Velocity of the RT Walker along heading direction.

shown in Fig. 4. Attaching the laser range finder at an angle to the horizontal plane allows detecting the positions of both the obstacles and the steps based on the measured distance.

If the distance d_H is constant, which is derived in advance based on the attached angle and height of the laser range finder from the ground level, it means that the walker is on flat ground. If the measured distance is larger than d_H, the RT Walker detects steps. When the measured distance is smaller than the constant distance d_H, the RT Walker detects obstacles.

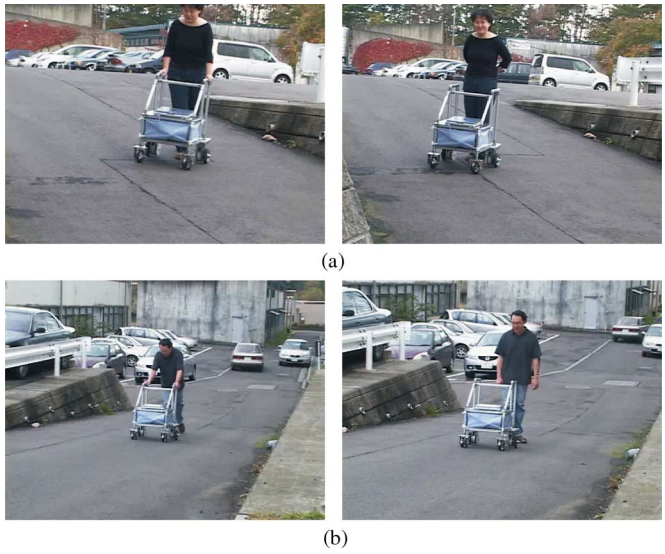

Fig. 16. Uphill and downhill experiments. Although the user did not touch the RT Walker, which was on a downhill road, gravity did not move it. (a) Experiments using the RT Walker going downhill. (b) Experiments using the RT Walker going uphill.

In this case, the virtual force/moment is derived from the measured length d_O to realize obstacle avoidance. When RT Walker detects a level difference, it generates map information based on the boundary position of the level difference, as shown in Fig. 5. Here, the length d_S does not change after detecting the edge of the step. By deriving the virtual force/moment based on the map, as shown in Fig. 5, the user avoids a misstep.

2) Motion Control Based on Gravity Compensation: In this section, we consider gravity compensation. If we compensate for gravity using the servo brakes, the walker will not move on a slope, unless the user applies intentional force/moment. Thus, the user could use the RT Walker as if it is always on a horizontal plane. Gravity compensation of the RT Walker is an important user safety function.

To realize gravity compensation, we must derive the brake torque based on the pitch angle α and roll angle β, as shown in Fig. 6. To obtain these angles, the RT Walker has two tilt angle sensors. When on a slope, as shown in Fig. 6, the gravity $\mathbf{G}$ is derived from the pitch angle α and the roll angle β.

Let the difference between the center of mass of the RT Walker and the axis of the rear wheels be r_{CoM}, since its center of mass is not exactly positioned at the middle of the rear wheel axis. The brake torque needed for compensating gravity $\tau_{\mathbf{b}}$ is expressed as

$$\tau_{\mathbf{b}} = \begin{bmatrix} f_b \\ n_b \end{bmatrix} = G = \begin{bmatrix} -mg \sin \alpha \\ -mg \cos \beta \times r_{\mathrm{CoM}} \end{bmatrix}. \quad (16)$$

From the derived brake torque $\tau_{\mathbf{b}} = [f_b, n_b]^T$, we can generate the brake torque for each wheel using (4), so that we can compensate for gravity, and the user can use the walker as if it is always on a horizontal road.

Fig. 17. Experiments in the real world, with stairs, obstacles, and a downward slope. The user wore a blindfold to prevent visual feedback.

V. Experiments

We experimented with the RT Walker to illustrate the validity of the proposed control algorithms and the performance of a passive intelligent walker using servo brakes.

A. Experiments for Human Adaptive Motion Control

In this experiment, the human adaptive motion control algorithm is implemented in the RT Walker without using the environmentally adaptive motion control algorithm. In the first experiment, we moved the RT Walker on a slope, as shown in Fig. 7. We specified three damping parameters with respect to the walker's heading direction ($D_d = 100, 150, 200$ N $\cdot$ s/m), while maintaining damping with respect to rotational direction. This simulates a user applying a constant force to the walker, and provides velocity responses as experimental results.

Under the assumption that the original inertia m, original damping D, and the tilt angle of the slope were known, when we specify the desired damping D_d, we can derive the velocity response of the RT Walker, as shown in Fig. 7. We can also calculate the actual damping $D_{\exp}$ from the velocity responses based on the experiments, which compare the desired damping D_d with the actual damping $D_{\exp}$, as shown in Fig. 8.

The velocity responses detected by the encoder system of the RT Walker are shown in Fig. 8, and the actual damping parameters $D_{\exp}$ calculated from Fig. 8 are shown in Table I. These results show that the actual damping $D_{\exp}$ is close to the desired damping D_d, and the motion characteristics of the RT Walker can be changed arbitrarily. Note that the theoretical velocity responses differ from the actual velocity responses before reaching a steady state. This may be caused by static or Coulomb friction, which are not considered in this experiment.

Next, we performed experiments with the RT Walker by changing the damping parameter with respect to the rotational direction, while keeping the damping parameter along the heading direction. In this experiment, we set the walker on a slope at an angle with respect to the gravity direction along the slope, and then, moved it based on the gravitational force. When we specify five damping parameters with respect to the rotational direction ($D_{\theta d} - D_\theta = -40, -20, 0, 20, 40$ N $\cdot$ m $\cdot$ s/rad), the RT Walker was moved as shown in Fig. 9, which is the path of the middle of the rear wheel axis. From Fig. 9, we can see that with a large damping parameter, the RT Walker moved straight compared to the motion with a small damping parameter, and the motion characteristics could be changed with respect to the rotational direction as well as the heading direction.

B. Experiments for Environmentally Adaptive Motion Control

This section describes the experiments to illustrate the validity of the environmentally adaptive motion control algorithms. First, we experimented with collision avoidance, which prevents falling due to steps. In this experiment, a human pushed the RT Walker just enough to move it. This allowed us to determine the validity of the proposed control algorithm easily and intuitively. The experiments are shown in Fig. 10, and the paths of the representative point and the center of the walker's axle are shown in Fig. 11. These results show that the RT Walker detects a wall and a step, and avoids them by using only brake control.

In the next experiment, we used the RT Walker in the environment shown in Fig. 12. We generated an artificial potential field by specifying the following parameters: $k = 20, \rho_0 = 0.9$ m. In this experiment, four university students used the RT Walker, and each wore a blindfold to prevent visual feedback. The experimental results, shown in Fig. 13, illustrate the path of the RT Walker detected by the encoder system. Four people successfully used the RT Walker without colliding with the wall.

We also experimented with a path leading from a start point to a destination. In this experiment, we generated an S-line path for the RT Walker using the artificial potential field with the parameters $k = 400$, $\rho_0 = 1.0$ m, which can generate the potential with a steep gradient. In this experiment, five university students with blindfolds operated the RT Walker. The results are

shown in Fig. 14, and the differences between the desired and actual paths were almost zero; path following was successfully achieved.

Next, we experimented with gravity compensation. The RT Walker was placed on a plate, as shown in Fig. 15(a). A fork lift tilted the plate. The walker's pitch and roll angles measured by the tilt angle sensors are shown in Fig. 15(b); the brake forces generated by the servo brake are shown in Fig. 15(c). The velocities of the RT Walker, detected by the encoders on the wheels, are shown in Fig. 15(d). Two arrangements of the RT Walker with respect to the tilted plate are investigated, as shown in Fig. 15. Both results showed that the RT Walker adjusted its brake force based on the angle changes, compensating for changes in the force of gravity.

We also tested the RT Walker in a real-world environment, as shown in Fig. 16. Although the user did not touch the walker, which was either on a downhill or uphill road, it did not move because of the force of gravity. That is, it only moved when the user intentionally applied force to it, just as if it was always on a horizontal road. Note that the RT Walker cannot pull the user against gravity when walking uphill, which makes it different from active walkers. This is the disadvantage of the passive walker. However, when walking uphill, the user's load is less, because the passive walker is relatively lightweight, and is not pulled downward by gravity.

In a final experiment, we used the RT Walker in a real-world environment with stairs, obstacles, and a down slope. A user wore a blindfold to prevent visual feedback, as shown in Fig. 17. From this experimental result, you can see that the user can safely use the RT Walker, and can depend on it for navigation even in a complicated environment.

VI. Conclusion

In this paper, we proposed a new intelligent walker, based on passive robotics, to help the elderly, handicapped, or blind people who have difficulty in walking. We developed a prototype walker, the RT Walker, which employs servo brakes. We also proposed motion control algorithms, which change the apparent dynamics of the passive intelligent walker, to adapt to the difficulties of the user and the environment.

Although this paper focused on realizing several important functions of intelligent walkers, such as human adaptive and environmentally adaptive controls, the estimation of the human situation and selection of the appropriate functions are critical in creating dependable walkers. If an intelligent walker can recognize the user's situation, it can select from several functions, such as obstacle/step avoidance, gravity compensation, variable motion characteristics, fall-prevention, etc. Thus, users who are not professionals of the intelligent systems can use them dependably and practically, without considering the functions of an intelligent walker. Toward this direction, we also proposed a method for selecting the appropriate functions in [15], in which the user situation is estimated based on the distance between the user and the walker.

In future work, we will consider the human adaptive and environmentally adaptive motion control algorithms in more detail to improve the maneuverability of the RT Walker. In addition, we will evaluate the validity of the RT Walker through comments from many people, including the elderly, handicapped, blind people, physical therapists, and medical doctors. We will improve the mechanisms and control algorithms of the RT Walker.

References

[1] M. Fujie, Y. Nemoto, S. Egawa, A. Sakai, S. Hattori, A. Koseki, and T. Ishii, "Power assisted walking support and walk rehabilitation," presented at the 1st Int. Workshop Humanoid Human Friendly Robot., Tsukuba, Japan, 1998.

[2] Y. Hirata, T. Baba, and K. Kosuge, "Motion control of omni-directional type walking support system "walking helper"," in *Proc. IEEE Workshop Robot Human Interactive Commun.*, 2003, pp. 85–90, Paper 2A5

[3] J. Manuel, H. Wandosell, and B. Graf, "Non-holonomic navigation system of a walking-aid robot," in *Proc. IEEE Workshop Robot Human Interactive Commun.*, 2002, pp. 518–523.

[4] A. M. Sabatini, V. Genovese, and E. Pacchierotti, "A mobility aid for the support to walking and object transportation of people with motor impairments," in *Proc. IEEE/RSJ Int. Conf. Intell. Robots Syst.*, 2002, pp. 1349–1354.

[5] H. Yu, M. Spenko, and S. Dubowsky, "An adaptive shared control system for an intelligent mobility aid for the elderly," *Auton. Robots*, vol. 15, no. 1, pp. 53–66, 2003.

[6] S. Kotani, H. Mori, and N. Kiyohiro, "Development of the robotic travel aid HITOMI," *J. Robot. Autom. Syst.,* vol. 17, pp. 119–128, 1996.

[7] K. Z. Haigh and H. A. Yanco, "Automation as caregiver: A survey of issues and technologies," in *Proc. AAAI 2002 Workshop Autom. Caregiver: Role Intell. Technol. Elder Care*, pp. 39–53.

[8] A. Goswami, M. A. Peshkin, and J. Colgate, "Passive robotics: An exploration of mechanical computation," (Invited paper)," in *Proc. IEEE Int. Conf. Robot. Autom.*, 1990, pp. 279–284.

[9] M. A. Peshkin, J. E. Colgate, W. Wannasuphoprasit, C. A. Moore, R. B. Gillespie, and P. Akella, "Cobot architecture," *IEEE Trans. Robot. Autom.*, vol. 17, no. 4, pp. 377–390, Aug. 2001.

[10] G. Wasson, P. Sheth, M. Alwan, K. Granata, A. Ledoux, and C. Huang, "User intent in a shared control framework for pedestrian mobility aids," in *Proc. 2003 IEEE/RSJ Int. Conf. Intell. Robots Syst.*, pp. 2962–2967.

[11] M. Alwan, P. Rajendran, A. Ledoux, C. Huang, G. Wasson, and P. Sheth, "Stability margin monitoring in steering-controlled intelligent walkers for the elderly," presented at the AAAI Fall 2005 Symp., Arlington, VA.

[12] A. J. Rentschler, R. A. Cooper, B. Blaschm, and M. L. Boninger, "Intelligent walkers for the elderly: Performance and safety testing of VA-PAMAID robotic walker," *J. Rehab. Res. Dev.*, vol. 40, no. 5, pp. 423–432, 2003.

[13] P. Prautsch, T. Mita, and T. Iwasaki, "Analysis and control of a gait of snake robot," *Trans. IEE Jpn.*, vol. 120-D, no. 3, pp. 372–381, 2000.

[14] O. Khatib, "Real-time obstacle avoidance for manipulators and mobile robots," *Int. J. Robot. Res.*, vol. 5, pp. 90–98, 1986.

[15] Y. Hirata, A. Muraki, and K. Kosuge, "Motion control of intelligent walker based on renew of estimation parameters for user state," in *Proc. 2006 IEEE/RSJ Int. Conf. Intell. Robots Syst.*, pp. 1050–1055.

Yasuhisa Hirata (M'00) received the B.E., M.E., and Ph.D. degrees in mechanical engineering from Tohoku University, Sendai, Japan, in 1998, 2000, and 2004, respectively.

From 2000 to 2006, he was a Research Associate in the Department of Bioengineering and Robotics, Tohoku University, where he has been an Associate Professor since 2006. From 2002 through 2004, he was a Researcher at the Precursory Research for Embryonic Science and Technology (PRESTO), Japan Science and Technology Agency (JST). His current research interests include intelligent control of multiple mobile robots in coordination, human–robot cooperation system, power assist system, and walking support system.

Dr. Hirata received the Young Investigator Excellence Award of the Robotics Society of Japan in 2001, the Best Paper in Robotics Award of the IEEE International Conference on Robotics and Biomimetics (ROBIO) in 2004, the Research Promotion Award of the Aoba Foundation for the Promotion of Engineering in 2004, the Japan Society of Mechanical Engineers (JSME) Award for the Best Paper in 2005, the Best Paper Award of the Robotics Society of Japan in 2005, and the Original Paper Award of the FANUC FA and Robot Foundation in 2006. He is a member of the Robotics Society of Japan and the JSME.

Asami Hara received the B.E. degree from Ibaraki University, Hitachi, Japan, in 2002, and the M.E. degree from Tohoku University, Sendai, Japan, in 2004, both in mechanical engineering.

She is currently a Research Staff Member in JTEKT Corporation, Kariya, Japan.

Ms. Hara is a member of the Robotics Society of Japan and the Japan Society of Mechanica Engineers.

Kazuhiro Kosuge (M'87–SM'00–F'06) received the B.S., M.S., and Ph.D. degrees in control engineering from Tokyo Institute of Technology, Tokyo, Japan, in 1978, 1980, and 1988, respectively.

From 1980 through 1982, he was a Research Staff in the Production Engineering Department, Nippon Denso Company, Ltd. (currently, DENSO Company, Ltd.). From 1982 through 1990, he was a Research Associate in the Department of Control Engineering, Tokyo Institute of Technology. From 1990 to 1995, he was an Associate Professor at Nagoya University. Since 1995, he has been with Tohoku University, Sendai, Japan, where he is currently a Professor in the Department of Bioengineering and Robotics.

Prof. Kosuge is an AdCom member of the IEEE Robotics and Automation Society. He was a Vice President of the IEEE Robotics and Automation Society from 1998 to 2001, a Member of the Board of the Trustees of the Robotics Society of Japan during 1993–1994 and during 2001–2002. He has also been a Steering Committee Vice-Co-Chair of the International Conference on Robotics and Automation (ICRA'95), Nagoya, Japan, the General Chair of the International Conference on Intelligent Robots and Systems (IROS 2004), Sendai. He received the Japan Society of Mechanical Engineers (JSME) Awards for the Best Papers in 2002 and 2005, and the Robotics Society of Japan (RSJ) Award for the Best Papers in 2005. He is a Fellow of the JSME and the Organization of American State's Foreign Trade Information System (SICE).